



## Efficient removal of hazardous malachite green dye from aqueous solutions using H<sub>2</sub>O<sub>2</sub> modified activated carbon as potential low-cost adsorbent: kinetic, equilibrium, and thermodynamic studies

Rahmat Ali<sup>a</sup>, Tahira Mahmood<sup>a,\*</sup>, Salah Ud Din<sup>b</sup>, Abdul Naeem<sup>a</sup>, Madeeha Aslam<sup>a</sup>, Muhammad Farooq<sup>a</sup>,

<sup>a</sup>National Center of Excellence in Physical Chemistry, University of Peshawar, Peshawar 25120, Pakistan, Tel. +92 3329266988; email: tahiramahmood@uop.edu.pk (T. Mahmood)

<sup>b</sup>Department of Chemistry, University of Azad Jammu and Kashmir, Muzaffarabad, Azad Kashmir, Pakistan

Received 17 November 2018; Accepted 20 January 2019

### ABSTRACT

This work is aimed at exploring the efficiency of a novel H<sub>2</sub>O<sub>2</sub> modified activated carbon (PA-AC-HO) prepared from used tea leaves (UTLs) for the removal of toxic cationic dye, malachite green (MG) from aqueous systems. The surface properties of PA-AC-HO were analyzed by FTIR spectroscopy, scanning electron microscopy (SEM), BET surface area (S<sub>BET</sub>), Boehm's titration and point of zero charge (pH<sub>PZC</sub>), thermogravimetric (TG/DTA) and X-rays diffraction (XRD) analysis. Results showed that PA-AC-HO has sufficient number of acidic functional groups and pH<sub>PZC</sub> value lies in the acidic region. The SEM study confirmed that the adsorbent external surface is highly porous with BET surface area of 1,097.68 (m<sup>2</sup> g<sup>-1</sup>) and total pore volume of 0.83 cm<sup>3</sup> g<sup>-1</sup>. Proximate-ultimate analysis showed high carbon and oxygen content of PA-AC-HO with amorphous nature. The adsorption characteristics of PA-AC-HO for the uptake of MG were studied by batch method. The dye uptake capacity and rate was found to increase with increasing contact time, dye initial concentrations and solution pH, but showed a decreasing trend with increasing salt ionic strength. Kinetic investigation revealed that adsorption of MG followed pseudo-second order model while the equilibrium isotherm data fitted the Langmuir and Temkin models well and maximum adsorption capacity was found to be 454.55 mg g<sup>-1</sup>. Thermodynamic investigation showed spontaneous and endothermic nature of the adsorption. Regeneration of dye loaded adsorbent was carried out by five consecutive cycles which showed good regeneration capacity.

*Keywords:* Activated carbon; H<sub>2</sub>O<sub>2</sub>; MG; Kinetic models; Isotherm models; Thermodynamics; Regeneration

### 1. Introduction

Water is the most vital element for existence of life on earth. But the ever growing population of the world and increasing industrial activities has resulted in the serious problem of water chemical pollution across the globe. Dyes is one of the major class of organic pollutants which are present in effluents of various industries, such as textiles, leather, plastics, printing, paper, cosmetics, pulp, paint,

pharmaceutical and food processing. The effluents from these industries which are extensively colored, containing heavy load of dyes along with other chemicals such as surfactants, waxes, aromatic compounds, pigments, color, suspended salts, heavy metals etc, are released into water bodies. The color which is a key indicator of water pollution interferes with penetration of sunlight into streams and causes a reduction in photosynthetic activity of aquatic plants that threaten ecological system [1–4]. Dyes molecules are highly

\* Corresponding author.

stable toward light and oxidizing agents and are difficult to biodegrade due to their complex aromatic structures. Most of the dyes and their metabolites are highly toxic, carcinogenic, mutagenic and cause serious problems to human health as well as aquatic organisms [2,5]. There are more than 1,00,000 dyes of various chemical structures existing commercially with an annual production of 7,00,000 metric tons per annum and about 10%–15% of these dyes are released without any proper treatment into water bodies [6].

Malachite green (MG) or Basic green 4 is a cationic triphenylmethane dye which has various scientific and industrial applications was selected as the targeted pollutant. It is widely used in textile coloring, leather, paper and plastics industries. It is also applied in manufacturing of paints, printing inks and as antifungal agent in aquaculture and fish breeding industry [7]. In addition to the commercial and social significance, MG is highly toxic to a wide range of aquatic and land animals. Experimental and clinical investigations showed that MG is a multi-organ toxin. It reduces food intake, growth rate and fertility in humans, damages respiratory system, liver, kidneys, heart and causes lesions on the skin and eyes. It is cytotoxic to mammalian cells and has potential carcinogenic, genotoxic and mutagenic properties [8]. In view of toxic nature, removal of MG from wastewater is very important and urgent need of the era to shield the ecosystem and human health.

Various treatment methods such as coagulation/flocculation, chemical oxidation, membrane technology, electrochemical degradation, photocatalytic degradation, microbiological decomposition and adsorption [4,9–11], have been generally employed for the detoxification of dyes bearing wastewater. Among these technologies, adsorption has been found to be the most effective physical process because of its high efficiency for a wide range of compounds, economic feasibility, easy availability and ease of operation [12–14]. A number of adsorbents have been used for decontamination of dyes bearing wastewater. However, activated carbon has been proved to be more efficient and promising adsorbent for non-biodegradable dyes removal from aqueous solutions. The use of activated carbon in most applications is related to its surface area, pore structure and various chemical functional groups present on the outer and inner surfaces [15]. The activated carbon formed during carbonization reactions may be apolar or with limited number of surface groups which reduces its wide spread application. This shortcoming can be overcome by modifying its surface by various chemical and physical methods. Chemical modification methods are most commonly used for obtaining activated carbon with hydrophilic surface which is related to the presence of various oxygen functional groups such as carboxylic, phenolic and lactonic groups on its surface. The type and amounts of these functional groups highly affect the adsorption efficiency of activated carbon [16].

Different oxidizing agents like  $\text{H}_2\text{O}_2$ ,  $\text{HNO}_3$ ,  $\text{O}_3$  and  $\text{KMnO}_4$  have been used to increase the amount of oxygen containing groups on activated carbon surface. Oxidation with these reagents increases the surface acidic functionality and enhances adsorption capacity of activated carbon for organic pollutants [16,17]. The efficiency of carbon based materials, modified with  $\text{H}_2\text{O}_2$  for adsorption of dyes and metal ions from aqueous solutions have been reported. Zuo

et al [18] showed that  $\text{H}_2\text{O}_2$  modification of hydrothermal biochar increased the number of carboxylic groups on its surface and correspondingly enhanced the capacity of biochar for heavy metal removal from aqueous solutions. Pereira et al [19] studied the adsorption properties of commercial activated carbon modified with  $\text{HNO}_3$ ,  $\text{H}_2\text{O}_2$ ,  $\text{NH}_3$  and thermal treatment under hydrogen flow. It was observed that the surface of activated carbon modified with  $\text{HNO}_3$ ,  $\text{H}_2\text{O}_2$  had increased number of oxygen containing acid groups which had positive effect on dyes uptake capacity with electrostatic and dispersion interactions as the dominant adsorption forces.

In the present study,  $\text{H}_2\text{O}_2$  which is an inexpensive and clean oxidizing agent has been used to modify the surface of activated carbon prepared from used tea leaves (UTLs). The adsorption capacity of the prepared adsorbent (PA-AC-HO) for the removal of toxic cationic dye, MG from synthetic wastewater was investigated. To the best of our knowledge, adsorption of MG using  $\text{H}_2\text{O}_2$  modified activated carbon as novel green adsorbent has not yet been reported. Emphasis was placed on probing mass transfer limitations, equilibrium, kinetic and thermodynamics aspects so as to find suitable mechanism for MG adsorption onto the surface of adsorbent. Desorption and regeneration was carried out to find the economic feasibility of adsorbent. Finally it is shown that PA-AC-HO can be a novel, economic and effective adsorbent for the uptake of MG from wastewater.

## 2. Experimental

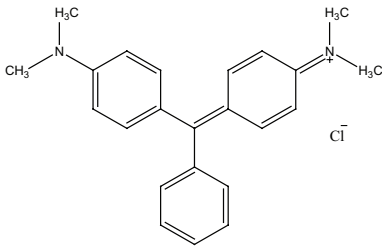
### 2.1. Chemicals and reagents

All the reagents/chemicals used in this research work were of high purity grade and were used without further purification. Hydrogen peroxide (30%), Sodium hydroxide pellets (99.99%), HCl (37%), NaCl (99%),  $\text{CaCl}_2$  (99%),  $\text{Al}_2\text{Cl}_3$  (95.1%),  $\text{Na}_2\text{CO}_3$  (99.5%),  $\text{NaHCO}_3$  (99.1%), were purchased from Scharlau, Spain. MG was supplied by Sigma Aldrich, Germany. The properties and structure of MG is shown in Table 1. Stock solution ( $1,000 \text{ mg L}^{-1}$ ) was prepared by dissolving accurately weighed quantity of the dye in double distilled water which was further diluted to obtain the solutions of desired concentration for conducting experiments.

### 2.2. Preparation of modified activated carbon

Activated carbon with  $S_{\text{BET}}$  of  $1,136.24 \text{ m}^2 \text{ g}^{-1}$  and total pore volume of  $0.86 \text{ cm}^3 \text{ g}^{-1}$ , obtained from used tea leaves (UTLs) under optimum conditions as reported in our previous work [20], was used as starting material for the preparation of modified activated carbon. Modification with  $\text{H}_2\text{O}_2$  was carried out by mixing 2 g of powder activated carbon (particles size of 0.15–0.5 mm) with 30 ml of  $\text{H}_2\text{O}_2$  (30 wt. %) solution taken in Erlenmeyer flask. The mixture was stirred for 24 h at 303 K. The supernatant was then separated by filtration and the residual solid was washed several times with double distilled water to remove any remaining  $\text{H}_2\text{O}_2$ . The sample was then dried at  $105^\circ\text{C}$  for 24 h and stored in air tight bottles for further analysis. This carbon sample was named as hydrogen peroxide modified activated carbon (PA-AC-HO).

Table 1  
Properties and structure of malachite green

C.I name	Basic Green 4
Commercial name	Malachite Green
Abbreviation	MG
IUPAC name	4-[[4-(dimethylamino) phenyl](phenyl) methylidene]-N,N-dimethylcyclohexa-2,5-dien-1-iminium chloride
Molecular formula	C <sub>23</sub> H <sub>25</sub> ClN <sub>2</sub>
Class	Triphenylmethane
Molar mass (g mol <sup>-1</sup> )	364.91
C.I No.	42000
Chemical class	Cationic
Ionization	Basic
λ <sub>max</sub> (nm)	618
Structure	

### 2.3. Adsorbent characterization

The surface area and porous structure of PA-AC-HO was measured by N<sub>2</sub> adsorption-desorption isotherms at -196°C using a surface area analyzer (ASAP-2010M+C, Micromeritics Instrument Corp., USA). BET surface area (S<sub>BET</sub>) was calculated by applying Brunauer, Emmett, and Teller equation to the adsorption data [20]. The total pore volume was determined by Berret-Joyner-Halenda (BJH) method from the amount of nitrogen adsorbed at P/P<sub>0</sub> 0.95 [21]. Micropore volume and micropore surface area was determined by Dubinin-Radushkevich (DR) equation [22]. The mesopore volume was calculated by subtracting the micropore volume from the total pore volume [23]. The surface morphology of PA-AC-HO was studied by scanning electron microscope (JEOL-JSM-5910, Japan) at 20 keV. Elemental analysis was carried out by Energy Dispersive X-ray (EDX) micro analyzer Spectrometer (INCA-200, UK) and CHNS analyzer (LECO CHNS-932, St. Joseph, USA). X-ray diffraction analysis was performed using JEOL X-ray diffractometer (model JDX-3532). Surface chemistry was studied by Fourier Transform Infrared (FTIR) spectrophotometer (FTIR-2000, PerkinElmer) and Boehm's titration method [24]. Proximate analysis was carried out according to the American Standard Testing Methods for materials, ASTM D1762-84. Point of zero charge (pH<sub>pzc</sub>) was measured by the well-defined drift method [25].

### 2.4. Batch adsorption studies

All the adsorption experiments were carried out by batch method in a series of 100 ml of polythene bottles containing a known amount of adsorbent and 40 ml of dye solution, placed in thermostatic shaker bath (SHEL LAB,

WS 17-2, USA) and agitated at a constant speed of 120 rpm for definite time. The solution pH was adjusted by addition of dilute solution of HCl or/and NaOH (0.1 M) by a pH meter (Neo Met, pH 250 L, Korea). The effect of various parameters such as pH, contact time, adsorbent dose, ionic strength, dye initial concentration and temperature on adsorption capacity of MG was evaluated. All the experiments were conducted in triplicate and the average value was used in data analysis. The dye residual concentration in solution was determined by UV-Vis spectrophotometer at the wavelength of its maximum absorbance (λ<sub>max</sub> 618 nm). The adsorption loading, q<sub>e</sub> (mg g<sup>-1</sup>) and percentage adsorption (%R) of dye were calculated using the following equation:

$$q_e = \frac{V(C_o - C_e)}{W} \quad (1)$$

$$\% R = \frac{(C_o - C_e)}{C_o} \times 100 \quad (2)$$

where C<sub>o</sub> and C<sub>e</sub> are the initial and equilibrium dye concentrations (mg L<sup>-1</sup>) in solution, V is the volume (L) and W is the weight of adsorbent.

### 2.5. Kinetics study

Adsorption kinetics studies were carried out to examine the effect of contact time, determine equilibrium point and kinetic parameters. A known amount of adsorbent (0.05 g) was taken in a series of 100 ml polythene bottles, containing 40 ml of dye solution of known concentration (100, 200, 300 and 400 mg L<sup>-1</sup>) and were placed in a thermostat shaker bath at 120 rpm and 298 K. At predetermined time intervals, the bottles were taken out of shaker bath, and the adsorbent particles were separated by centrifugation from the solutions and analyzed for dye uptake at the corresponding λ<sub>max</sub>.

### 2.6. Adsorption isotherm study

Equilibrium isotherm experiments were performed by contacting 40 ml of dye solutions of different initial concentration (100–1,000 mg L<sup>-1</sup>) with 0.05 g of PA-AC-HO at fixed temperature (293, 303, 313 and 323 K). The pH of the solutions was adjusted to the desired pH values and shaken for maximum contact time required to attain equilibrium, as determined from the kinetic experiments. The amount of dye adsorbed was calculated using Eq. (1). The equilibrium data were modeled using Langmuir, Freundlich, Temkin and Dubinin-Radushkevich (D-R) isotherm equations.

### 2.7. Desorption and regeneration of adsorbent

Desorption and regeneration studies were carried out to investigate the efficiency and reusability of PA-AC-HO. A known amount (0.05 g) of dye loaded adsorbent was immersed in 40 ml of the desorbing medium and agitated in shaker bath for 4 h under the same conditions as used in the adsorption experiments. Thereafter, the concentration of

dye desorbed was measured and the adsorbent collected was washed and reused again. The percentage of dye desorbed (Desorption efficiency,  $D$ ) was determined by the following equation:

$$D\% = \frac{C_d}{C_o - C_e} \times 100 \quad (3)$$

where  $C_o$  and  $C_e$  are the initial and equilibrium concentrations ( $\text{mg L}^{-1}$ ) of dye in solution and  $C_d$  is the concentration ( $\text{mg L}^{-1}$ ) of dye at equilibrium after desorption.

### 3. Results and discussion

#### 3.1. Characterization of adsorbent

##### 3.1.1. Textural analysis

The specific surface area ( $S_{\text{BET}}$ ) and pore volume of PA-AC-HO was determined from  $\text{N}_2$  adsorption-desorption isotherms and the values obtained are listed in Table 2. Results show that the adsorbent surface is highly porous with good BET surface area and have considerable amount of micropores. However, modification with  $\text{H}_2\text{O}_2$  which is an oxidizing agent leads to a significant decrease in the  $S_{\text{BET}}$  and micropore-volume with a major increase in mesopore volume. The BET surface area and Micropore volume of the precursor activated carbon was decreased respectively from 1,136 to 1,097.68  $\text{m}^2 \text{g}^{-1}$  and 0.47 to 0.35  $\text{cm}^3 \text{g}^{-1}$  in PA-AC-HO. The fraction of mesopore volume was increased from 45.35% to 57.83%. This reduction in micropore volume which is accessible to adsorption of nitrogen at 77 K, with the corresponding increase in mesopore volume can be related to collapse and destruction of pore walls and development of some oxygen surface groups on the entry or on the walls of micropores [26,27].

##### 3.1.2. Surface morphology and X-Ray diffraction (XRD) analysis

The SEM micrographs of PA-AC-HO before and after adsorption are presented in Fig. 1(a) and (b), respectively. It can be observed from these micrographs that the external surface of PA-AC-HO is highly porous with some carcks, which may be due to the destruction of the pore walls and widening of the micropores after modification with  $\text{H}_2\text{O}_2$ . Surface modification with  $\text{H}_2\text{O}_2$  results in a considerable

decrease in specific surface area and pore volumes of PA-AC-HO. This well-developed porous structure was responsible for higher uptake of MG from aqueous solutions. The surface of PA-AC-HO (Fig. 1(b)) after dyes adsorption has been changed with some of the pores disappeared. This may be due to the saturation and pore filing by the dye molecules.

X-Ray diffraction (XRD) analysis is a powerful tool to evaluate the crystalline structure of material. The XRD spectrum of PA-AC-HO (Fig. 1(c)) showed amorphous nature of adsorbent, which is an important characteristic of porous adsorbent. A broad diffraction peak at angle  $2\theta$  of about  $25^\circ$  was observed which correspond to (002) plane of amorphous graphitic carbon [17].

##### 3.1.3. Surface chemistry

The FTIR spectra of PA-AC-HO before and after dyes uptake are presented in Fig. 1(d). The bands around 3,000–3,732 indicate the presence of O–H stretching vibration of carboxylic, phenolic and of aliphatic alcoholic groups [28,29]. The weak and medium peak at 3,026  $\text{cm}^{-1}$  correspond to =C–H stretching in alkene while the peaks at band width of 2,800–2,883  $\text{cm}^{-1}$  were assigned to C–H stretching vibration of alkanes and alkyl groups. The band at 2,334  $\text{cm}^{-1}$  region corresponds to C≡C vibrations in alkyne and methylene groups. The weak peaks at 1,837–1,691  $\text{cm}^{-1}$  were assigned to C=O stretching vibration of carbonyl and carboxylic groups [30]. The band in the region of 1,500–1,551  $\text{cm}^{-1}$  was attributed to bond vibrations of an aromatic species and C–O axial deformation [31]. The peaks around 1,306 show the presence of C–N stretching in aromatic tertiary amines. The absorption bands at 1,227  $\text{cm}^{-1}$  may be due to phenolic O–H groups and the peak around 1,070  $\text{cm}^{-1}$  indicates the presence of C–O stretching in primary alcohols. The peaks at 892–834 are attributed to –OC–OH vibration and 763–641  $\text{cm}^{-1}$  indicate C–H out-of-plane bending in an aromatic ring [30]. FTIR studies revealed that after the uptake of MG the absorption bands at 3,732, 3,042, 2,890, 2,334, 1,537, 1,330, 1,227, 1,070 and 892  $\text{cm}^{-1}$  had correspondingly shifted to 3,712, 3,026, 2,883, 2,300, 1,551, 1,306, 1,212, 1,060 and 834  $\text{cm}^{-1}$  which may be due to the binding of dye molecules to the adsorbents surfaces by Vander Waals and electrostatic interactions. These recommended that PA-AC-HO could be used as an efficient adsorbent for dyes removal from aqueous systems.

Table 2  
Textural and surface chemical properties of PA-AC-HO

Textural properties						
Surface area ( $S_{\text{BET}}$ ), ( $\text{m}^2 \text{g}^{-1}$ )	Micropore surface area (DR), ( $\text{m}^2 \text{g}^{-1}$ )	Micropore volume (DR), ( $\text{cm}^3 \text{g}^{-1}$ )	Mesopore volume ( $\text{cm}^3 \text{g}^{-1}$ )	Total pore volume (BJH), ( $\text{cm}^3 \text{g}^{-1}$ )	Fraction, % (micropore)	Fraction, % (mesopore)
1097.68	629.92	0.35	0.48	0.83	42.17	57.83
Acidic functional groups ( $\text{mmol g}^{-1}$ )					Basic groups ( $\text{mmol g}^{-1}$ )	$\text{pH}_{\text{PZC}}$
Carboxylic	Lactonic	Phenolic	Carbonyl	Total acidic groups		
1.94	0.96	1.68	0.05	4.63	0.04	3.40

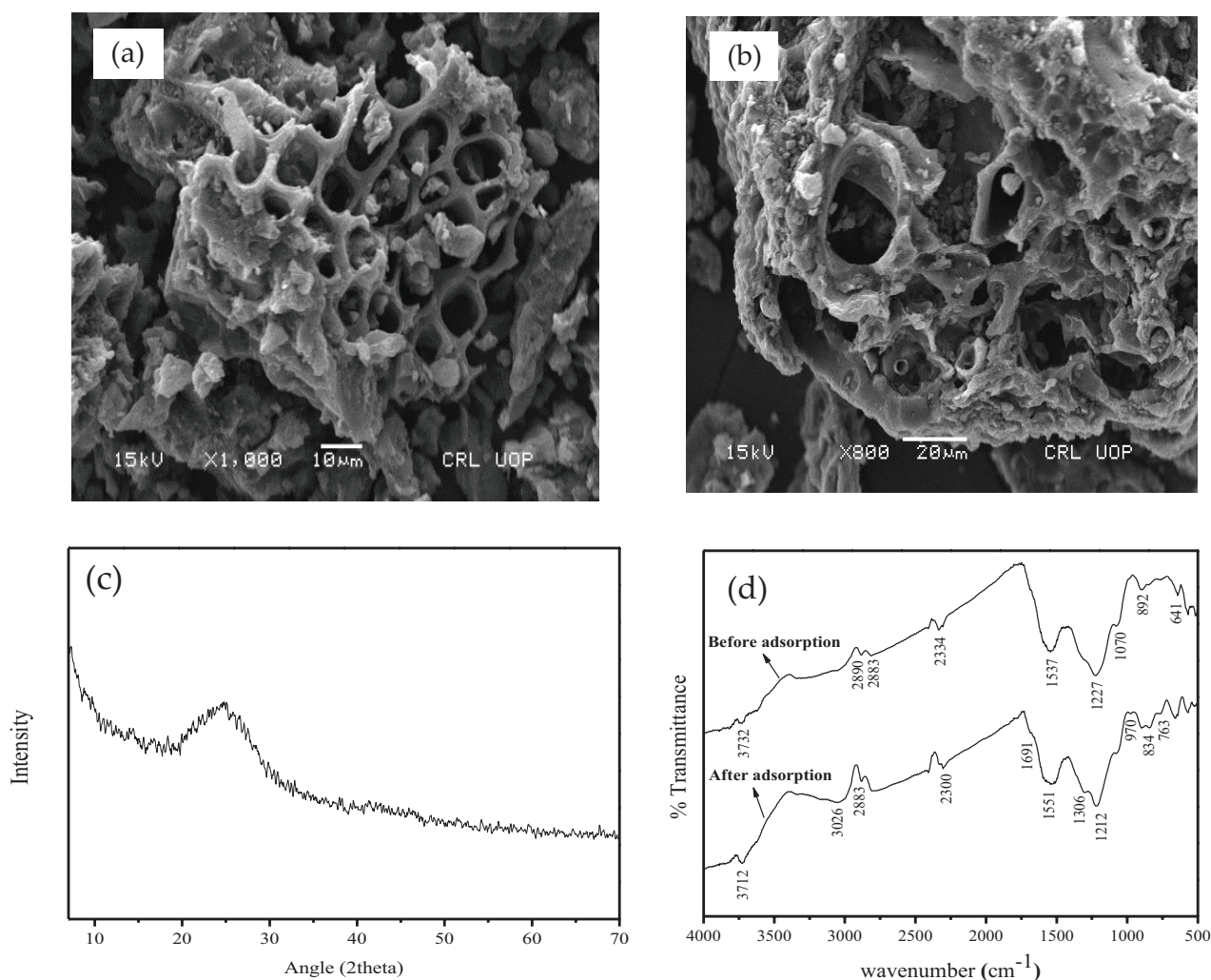


Fig. 1. Scanning electron micrograph (a) before adsorption, (b) after adsorption, (c) X-rays diffraction pattern and (d) FT-IR spectra of PA-AC-HO.

#### 3.1.4. Boehm's titration and $pH_{pzc}$

Boehm's titration results revealed that PA-AC-HO has considerable amount of carboxylic and phenolic groups with relatively less number of lactones groups (Table 2). Total acidic groups was found to be  $4.63 \text{ mmol g}^{-1}$  which is markedly higher than its total basic groups ( $0.04 \text{ mmol g}^{-1}$ ) and thus showed acidic surface nature of adsorbent which is also supported by its  $pH_{pzc}$  value (3.40). It has been reported [27,32] that modification of activated carbon with  $H_2O_2$  increase the number of acidic groups which is also accompanied by a slight decreased in the total surface area and micropore volume due to the presence of surface oxygen groups on the pores walls.

#### 3.1.5. Proximate-ultimate and EDX analysis

The proximate-ultimate analysis of PA-AC-HO was carried out by ASTM techniques (ASTM-D1762-84), and the results acquired are given in Table 3. It is evident that PA-AC-HO possessed a low ash contents and higher amount of fixed carbon which make it high-quality adsorbent for

adsorption of organic pollutants from aqueous systems. Ultimate analysis (Table 3) indicated that PA-AC-HO has higher oxygen content (26.52%) than its precursor activated carbon (16.24%). The increase in oxygen content may be due to oxidation of precursor activated carbon during modification with  $H_2O_2$ . The percentage of various elements obtained from EDX spectra are given in Table 3. The major elements evaluated by EDX analysis are C, O, P and N with trace amounts of Ca and Cu which depending on the nature and origin of the precursor and also on the post treatment of prepared sample. The EDX analysis also confirmed that after modification with  $H_2O_2$ , the oxygen content of PA-AC-HO (17.06%) was increased compared with precursor activated carbon (11.36%). This investigation is similar to the results of previous studies that modification of activated carbon with  $H_2O_2$  can cause oxidation of its surfaces and enhance the oxygen functionalities of the surfaces [26]. The presence of phosphorus may be due to the presence of stable complexes such as  $C_3P$ ,  $COPO_3$  and  $CPO_3$  at the carbon surface, formed by the reaction of phosphoric acid with the precursor material during activation process [33].

### 3.2. Adsorption studies

#### 3.2.1. Effect of solution pH

The adsorption of MG on the surface of PA-AC-HO was studied as a function of pH at 298 K in the pH range of 2–10 with initial concentration of 200 mg L<sup>-1</sup> as shown in Fig. 2(a). It can be seen that the percent adsorption was low in the pH range of 2.0–4.0. A marked increase in percent adsorption was observed with increasing solution pH from 4.0 to 7.0, indicating that MG adsorption is more feasible at high pH value. However, no significant increase in percentage adsorption was observed on further increasing pH value from 7.0 to 10.0. Optimum adsorption was observed at pH 7.0, therefore further adsorption studies were carried

out at pH 7.0. Dyes uptake is highly dependent on the type and ionic state of the surface functionalities and also on the chemistry of dyes in solution. The  $pH_{pzc}$  value for PA-AC-HO was found to be 3.40 (Table 2). At  $pH < pH_{pzc}$ , PA-AC-HO surface may take H<sup>+</sup> ions from solution and get positively charged through protonation of phenolic and carboxyl groups present on the surface according to Eqs. (4) and (5). This result in electrostatic repulsion between the PA-AC-HO surface and dye cations and hence results in lower percentage adsorption. However, at  $pH > pH_{pzc}$ , PA-AC-HO surface becomes negatively charged due to deprotonation of surface groups as given by Eqs. (6) and (7). Hence at high pH values adsorption of MG<sup>+</sup> cations is preferred due to increasing electrostatic attraction [34].

Table 3  
Proximate-ultimate and EDX analysis of PA-AC-HO

Proximate analysis (dry basis, wt %)				Ultimate analysis (dry basis, wt %)			
Moisture	Volatile	Ash	Fixed carbon	C	H	N	O
3.16	9.23	6.37	81.24	70.39	1.88	1.21	26.52
Weight % of different elements by EDX analysis before adsorption							
C	N	O	P	Ca	Cu	Mg	Total
72.55	Nil	17.06	8.36	1.09	0.94	Nil	100
Weight % of different elements by EDX analysis after adsorption							
C	N	O	P	Ca	Cu	Mg	Total
82.76	Nil	13.98	3.25	Nil	Nil	Nil	100

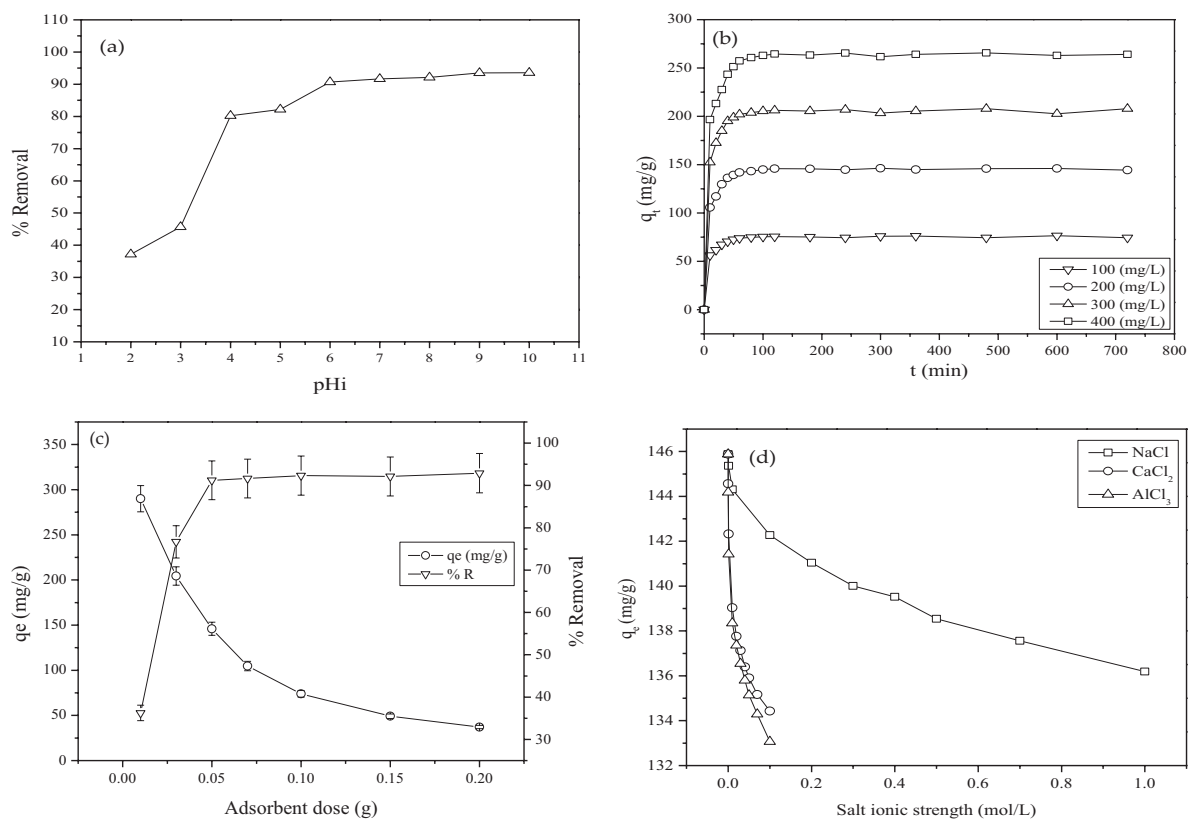
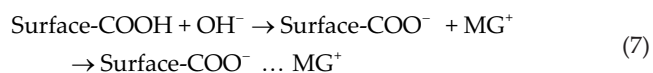
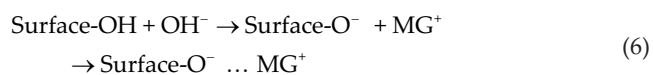
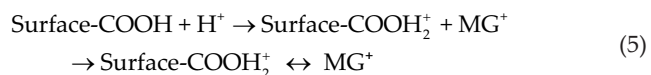
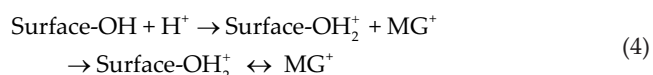


Fig. 2. (a) Effect of solution pH and (b) Contact time and dye initial concentration, (c) Adsorbent dosage and (d) Salts (NaCl, CaCl<sub>2</sub>, 2H<sub>2</sub>O and AlCl<sub>3</sub>·6H<sub>2</sub>O<sub>2</sub>) ionic strength on MG adsorption by PA-AC-HO at 298 K and pH 7.0.



### 3.2.2. Effect of contact time and dye initial concentration

The effect of contact time on the uptake of MG by PA-AC-HO was studied at different initial concentration (100–400 mg L<sup>-1</sup>) at pH 7.0, 298 K and constant adsorbent dose (0.05 g) as can be seen in Fig 2(b). It is evident from the figure that the amount of dye adsorbed per unit mass of adsorbent is highly dependent on contact time and dye initial concentration. The adsorption was rapid at initial contact time and then gradually decreased until the point of saturation is reached. The adsorption equilibrium was established in about 120 min at all studied concentrations. The high adsorption capacity at initial stages may be due to the presence of more active sites on adsorbent surfaces. The active sites then tend to decrease rapidly with time as the adsorption precedes which results in slow adsorption rate and ultimately reaches a constant value. The slow adsorption rate at later stages may be due to the slow pore diffusion of dye cations into bulk of adsorbent as well as the electrostatic repulsion between the positively charged dye molecules adsorbed onto the surface of PA-AC-HO and the positively charged dye cations in solution [3]. The effect of MG initial concentration can also be seen in Fig 2(b). It was found that as the initial concentrations was increased from 100 to 400 mg L<sup>-1</sup>, adsorption capacity of MG at equilibrium was increased from 75.47 to 264.53 mg g<sup>-1</sup>. The increase in adsorption capacity with increasing dye concentration may be due to increase in number of collisions between dye cations in solution and the adsorbent surface and development of driving force of concentration gradient, that reduce all mass transfer resistances arises between the dye cations in solution and the solid phase [35].

### 3.2.3. Effect of adsorbent dose

Adsorbent dose is a major parameter as it investigates the sorption capacity of an adsorbent for any given adsorbate concentration. Therefore, it is very important to optimize the adsorbent dose for adsorption of various pollutants from aqueous solutions. The influence of adsorbent dose on the uptake of MG was studied by varying PA-AC-HO mass from 0.01 to 0.2 g with dyes initial concentration of 200 mg L<sup>-1</sup> at 298 K as shown in Fig. 2(c). As can be seen the percent removal of MG increases with increasing PA-AC-HO dose which may be due to the rise in surface area and availability of abundant

vacant sites on adsorbent surface [36]. The percent removal of MG was increased from 36.26% to 92.90% with increasing adsorbent dose from 0.01 to 0.2 g. However, the adsorption capacity ( $q_e$ ) was found to decrease with increasing adsorbent dosage. As an appreciable removal (about 91.22%) was achieved with PA-AC-HO dose of 0.05 g and only small increase was observed beyond this much amount. Therefore, 0.05 g was used as the optimum dose for further adsorption experiments.

### 3.2.4. Effect of ionic strength

The dyes containing wastewater usually contains different salts and metal ions. These salts due to their high ionic strength, can significantly affect the adsorption capacity of adsorbents. The effect of ionic strength on the adsorption of MG onto PA-AC-HO was studied by using NaCl (monovalent salt) solutions with concentration from 0.001 to 1.0 mol L<sup>-1</sup>, CaCl<sub>2</sub> (divalent salt) and AlCl<sub>3</sub> (trivalent salt) solutions both with concentrations from 0.0001 to 0.1 mol L<sup>-1</sup> and the results obtained are presented in Fig. 2(d). It can be observed that the adsorption capacity of MG was found to decrease with increasing salts concentrations. As NaCl, CaCl<sub>2</sub>, and AlCl<sub>3</sub> releases Na<sup>+</sup>, Ca<sup>2+</sup> and Al<sup>3+</sup> ions in dye solution, which may screen the electrostatic interaction between dye cations and the opposite charges at the surface of adsorbent and thus results in the reduction of MG adsorption capacity with increasing ionic strength. The degree of screening caused by the added salts is related to the size and valence of the metal ion [37,38]. The ions with small size are hydrated to smaller extent and the less hydrated ions are more closely attracted to the charged surface because of their smaller radii. Similarly, the ions with higher valence interact to a larger extent with the oppositely charged surface, causes screening of MG adsorption on PA-AC-HO. Hence, the extent of screening by added salts followed the order: Al<sup>3+</sup> > Ca<sup>2+</sup> > Na<sup>+</sup>. In the presence of Na<sup>+</sup> ions in solution MG adsorption capacity was reduced from 145.88 to 136.19 mg g<sup>-1</sup> with increasing NaCl concentration from 0.0 to 1.0 mol L<sup>-1</sup> while in the presence of Ca<sup>2+</sup> and Al<sup>3+</sup> ions MG uptake capacity was decreased to 134.43 and 133.07 mg g<sup>-1</sup> respectively, with increasing CaCl<sub>2</sub> and AlCl<sub>3</sub> concentration from 0.0 to 0.1 mol L<sup>-1</sup>. The decrease in MG uptakes with increasing salt concentration may be due to the competition among dye cations and Na<sup>+</sup>, Ca<sup>2+</sup> and Al<sup>3+</sup> ions for the existing binding sites. The affinity of dye cations for the available binding sites decreases with increasing ionic strength which results in the reduction of MG uptakes at the PA-AC-HO surface [38].

### 3.2.5. Adsorption kinetics and mechanism of adsorption

Adsorption kinetics explains the rate of solute uptake at the solid-solution interface and obviously provides useful information about the pathways and mechanism of adsorption process. The adsorption kinetics and mechanism of MG adsorption onto PA-AC-HO at four different concentration (100, 200, 300 and 400 mg L<sup>-1</sup>) were analyzed by using pseudo first order, pseudo second order, Elovich and intra-particle diffusion models.

The linearized form of Lagergren pseudo first order model is usually represented by the following equation:

$$\log(q_e - q_t) = \log q_e - \left( \frac{K_1}{2.303} \right) t \quad (8)$$

where  $q_e$  and  $q_t$  are the amounts of dye adsorbed ( $\text{mg g}^{-1}$ ) at equilibrium and at time  $t$  (min), respectively and  $k_1$  ( $\text{min}^{-1}$ ) is pseudo first order rate constant.

The rate equation for pseudo second order kinetic model is expressed as:

$$\frac{dq_t}{dt} = K_2(q_e - q_t)^2 \quad (9)$$

where  $k_2$  is the pseudo second order rate constant ( $\text{g mg}^{-1} \text{min}^{-1}$ ). For the boundary conditions,  $q_t = 0$  at  $t = 0$  and  $q_t = q_e$  at  $t = t$ , the integrated form of Eq. (9) will be as:

$$\frac{t}{q_t} = \frac{1}{k_2 q_e^2} + \frac{1}{q_e} t \quad (10)$$

The initial adsorption rate,  $h$  ( $\text{mg g}^{-1} \text{min}^{-1}$ ), at  $t \rightarrow 0$  is given as:

$$h = k_2 q_e^2 \quad (11)$$

The linear form of Elovich model [39] is:

$$q_t = \frac{1}{\beta} \ln(\alpha\beta) + \frac{1}{\beta} \ln t \quad (12)$$

where  $\alpha$  ( $\text{mg g}^{-1} \text{min}^{-1}$ ) is the initial adsorption rate,  $\beta$  ( $\text{g mg}^{-1}$ ) is related to the extent of surface coverage and activation energy.

The pseudo-first order, pseudo-second order and Elovich kinetic model plots for the adsorption of MG onto PA-AC-HO at different initial concentrations are given in Figs. 3(a)–(c). The values of  $q_e$ , rate constant  $k_1$ ,  $k_2$ ,  $\alpha$ ,  $\beta$  and correlation coefficient  $R^2$  obtained from the above plots using Eqs. (8), (10) and (12), are listed in Table 4. The pseudo-first order and Elovich model do not fit well the adsorption data with lower value of correlation coefficients ( $R^2$ ). The data points for pseudo-second order kinetic model fitted very well to straight line with high correlation coefficients ( $R^2 > 0.999$ ), and the  $q_e$  calculated from pseudo-second order model were in close agreement with the experimentally determined adsorption amount ( $q_{e,\text{exp}}$ ) as compared with pseudo-first order model at all the studied concentrations. It can also be seen from Table 4 that the values of rate constant  $k_2$  rises as dye concentration was increased from 100 to 400  $\text{mg L}^{-1}$  which may be due to limited number of active sites on PA-AC-HO surface. Moreover, initial adsorption rate ( $h$ ) increases with increasing initial dye concentration from 100 to 400  $\text{mg L}^{-1}$  and the highest value was obtained at 400  $\text{mg L}^{-1}$ , which may be due to the increase in mass transport driving force resulted from higher ratios of dye cations to the available active site on the surface of PA-AC-HO. These investigation shows that the uptake of MG by PA-AC-HO follows pseudo-second

order kinetic model. Similar results have been reported by Daneshvar et al for methylene blue biosorption using modified macroalgae [40].

### 3.2.6. Mass transfer mechanism

The kinetics of dyes adsorption on porous solid adsorbents is usually controlled by different mechanisms. The Weber and Morris intra-particle diffusion and Boyd's models are the most commonly used models for investigating the mechanism of dyes adsorption. Therefore, the experimental kinetic results were studied further by using these models, to confirm whether the adsorption process is controlled by film diffusion or particle diffusion.

Intra-particle diffusion model is generally used to verify the impact of mass-transfer resistance on the uptake of dye cations by the adsorbent surface and to evaluate the rate limiting step. The intra-particle diffusion model can be expressed by the following equation:

$$q_t = k_{\text{id}} t^{1/2} + C \quad (13)$$

where  $k_{\text{id}}$  is the intra-particle diffusion rate constant ( $\text{mg g}^{-1} \text{min}^{-1/2}$ ) and  $C$  is the intercept ( $\text{mg g}^{-1}$ ), related to the boundary layer thickness.

The values of  $k_{\text{id}}$  and  $C$  calculated from the slope and intercept of the plots of  $q_t$  versus  $t^{1/2}$  (Fig. 3(d)) are listed in Table 4. The larger the value of  $C$ , the greater will be the boundary layer effect [41]. It can be observed (Fig. 3(d)) that the adsorption of MG followed three steps process. The first portion was attributed to the rapid adsorption of dye cations from solution on to the external surface of adsorbent due to the presence of large number of active sites which is controlled by film diffusion (boundary layer diffusion). The second portion was the slower uptake, correspond to intra-particle diffusion. The third portion corresponds to the equilibrium stage, where the active sites become saturated with dye cations [35]. As dye cations migrate slowly into the pores by intra-particle diffusion. Therefore, intra-particle diffusion is the rate limiting step with  $k_{\text{id},2}$  values of the second portion are smaller than  $k_{\text{id},1}$  of the first portion of the plots of  $q_t$  versus  $t^{1/2}$ . The values of  $C$  increased with rising dye initial concentrations from 100 to 400  $\text{mg L}^{-1}$  at 298 K. This indicated that the boundary layer diffusion effect increases with increasing dye initial concentrations. However, the intra-particle diffusion is not only the rate limiting step as the plots of  $q_t$  vs.  $t^{1/2}$  did not have zero intercepts and did not pass through the origin with low  $R^2$  values. Therefore, it may be concluded that during the interaction of MG with PA-AC-HO both surface adsorption (film diffusion or boundary layer) and intra-particle diffusion may occurred parallel.

The fact that the particle diffusion is not only the rate controlling step in the overall sorption process was further confirmed by applying Boyd model to the kinetic data [42] and the various parameters were determined from the following equations:

$$F = 1 - \frac{6}{\pi^2} \exp(-Bt) \quad (14)$$



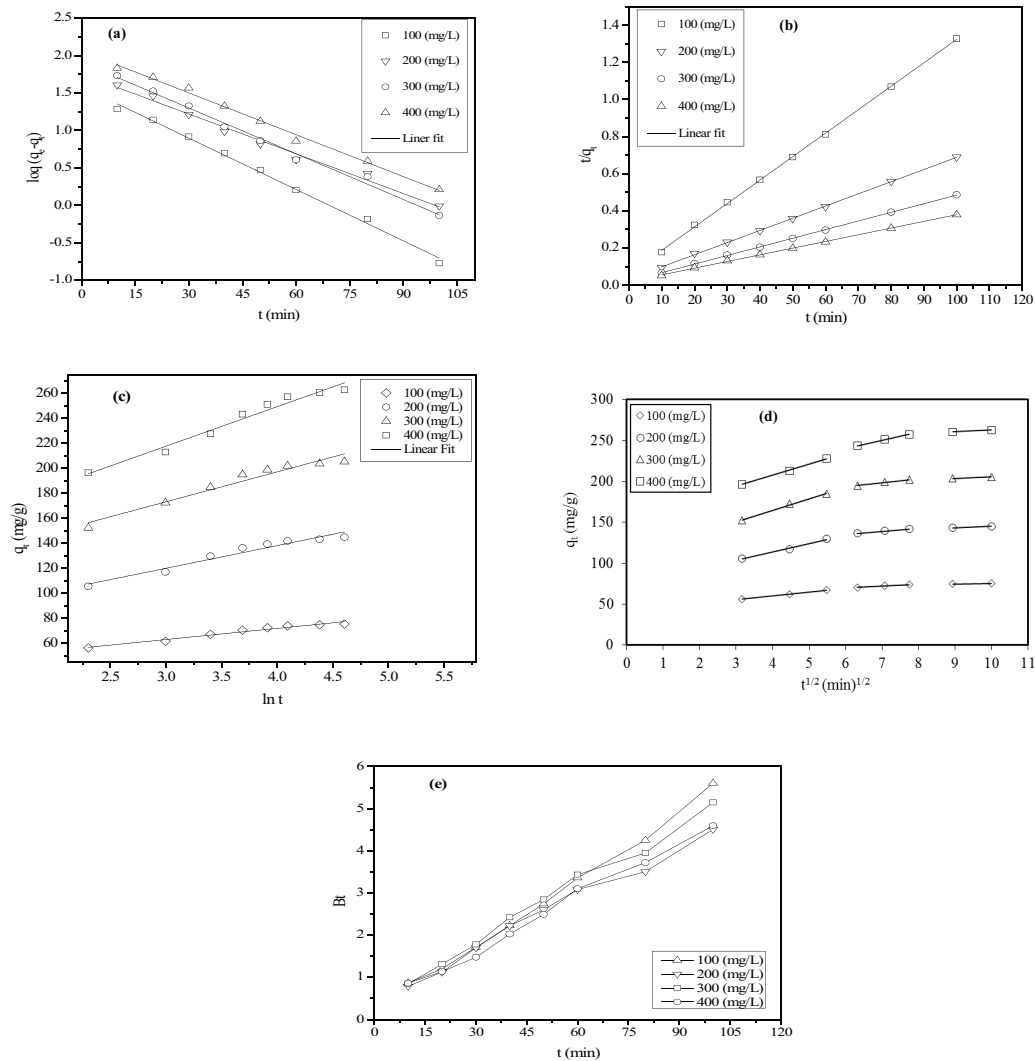


Fig. 3. (a) Pseudo first order, (b) Pseudo second order, (c) Elovich, (d) Intra-particle diffusion and (e) Boyd model plots for the adsorption of MG onto PA-AC-HO; dosage = 0.05 g/40 ml, pH, 7.0, dye initial Concentration = 100–400 mg L<sup>-1</sup>, Temperature = 298 K, and speed = 120 rpm.

where 'F' is the fractional adsorbate molecules adsorbed at any time 't', and can be evaluated as  $F = q_t/q_e$  while 'Bt' is a mathematical function of F. Eq. (14) can be rearranged as:

$$Bt = -0.4.977 - \ln(1 - F) \tag{15}$$

The Bt values were determined from Eq. (15) and were plotted against t as shown in Fig. 3(e). The mechanism of adsorption can be decided from Bt vs. t plots, whether it is particle diffusion or film diffusion controlled. If the plot of Bt vs. t is straight line with zero intercept, then the adsorption will occur by particle diffusion, otherwise it is controlled by film diffusion [42]. It can be observed from Fig. 3(e) that the plots of Bt vs. t for the adsorption of MG onto PA-AC-HO are linear in the initial time intervals only and did not pass through the origin for all studied concentrations, confirming that film diffusion is the rate controlling process in the initial stages of adsorption which is then followed by intra-particle diffusion.

### 3.2.7. Adsorption equilibrium study

Equilibrium isotherm study provides information about adsorption mechanism and the surface properties of adsorbent [43]. The equilibrium isotherms for the adsorption of MG onto PA-AC-HO at 293, 303, 313 and 323 K over a wide concentration range (100–1,000 mg L<sup>-1</sup>) at pH 7.0 are shown in Fig. 4(a). It can be seen that the amount of dye adsorbed ( $q_e$  (mg g<sup>-1</sup>)) increases slightly with increasing temperature from 293 to 323 K. Moreover; the isotherms are concave presenting a saturation tendency with increasing dye concentration. To further study, the behavior of MG adsorption, the equilibrium data were analyzed by the Langmuir, Freundlich, Temkin and Dubinin-Radushkevich (D-R) isotherm models.

The Langmuir model assumes that the adsorption of sorbate species occurs by monolayer adsorption on a homogeneous surface with a fixed number of adsorption sites of uniform energies. The linear form of Langmuir isotherm model can be represented as follows:

Table 4

Kinetic and intra-particle diffusion model parameters for adsorption of MG onto PA-AC-HO at 298 K with different initial concentrations at pH 7.0

Model	Parameter	$C_o$ (mg L <sup>-1</sup> )			
		100	200	300	400
Pseudo-first order	$q_{e,cal}$ (mg g <sup>-1</sup> )	38.33	56.29	81.39	114.92
	$k_1$ (10 <sup>-3</sup> ) (min <sup>-1</sup> )	50.66	40.76	46.98	42.83
	$R^2$	0.98	0.98	0.99	0.98
Pseudo-second order	$q_{e,exp}$ (mg g <sup>-1</sup> )	75.47	145.94	206.17	264.53
	$q_{e,cal}$ (mg g <sup>-1</sup> )	79.36	151.51	217.39	277.78
	$k_2$ (10 <sup>-3</sup> ) (g mg <sup>-1</sup> min <sup>-1</sup> )	2.59	1.32	1.04	0.67
	$h$ (mg g <sup>-1</sup> min <sup>-1</sup> )	16.34	30.39	49.02	51.55
	$R^2$	0.999	0.999	0.999	0.999
Elovich	$\alpha$ (mg g <sup>-1</sup> min <sup>-1</sup> )	521.00	675.22	1661.23	1537.48
	$\beta \times 10^{-2}$ (g mg <sup>-1</sup> )	11.22	5.51	4.18	3.16
	$R^2$	0.96	0.95	0.95	0.97
Intra-particle diffusion	$k_{id,1}$ (mg g <sup>-1</sup> min <sup>-1</sup> )	4.69	10.32	14.14	13.42
	$C_1$ (mg g <sup>-1</sup> )	41.22	72.38	108.18	153.80
	$R_1^2$	0.99	0.99	0.99	0.99
	$k_{id,2}$ (mg g <sup>-1</sup> min <sup>-1</sup> )	2.37	3.91	4.98	9.81
	$C_2$ (mg g <sup>-1</sup> )	55.62	111.62	163.56	181.49

$$\frac{C_e}{q_e} = \frac{1}{K_L q_{max}} + \frac{C_e}{q_{max}} \quad (16)$$

where  $q_{max}$  is the maximum theoretical monolayer adsorption capacity (mg g<sup>-1</sup>) and  $K_L$  is the Langmuir constant correspond to the affinity of sorption sites (L mg<sup>-1</sup>). The values of the Langmuir constants,  $q_{max}$  and  $K_L$  were determined from the slopes and intercepts of  $C_e/q_e$  vs.  $C_e$  plots (Fig. 4(b)), respectively and are listed in Table 5. The value of  $R^2$  was found to be greater than 0.99 at all the studied temperatures, showing the fitness of Langmuir isotherm model with monolayer coverage on PA-AC-HO surface. The higher value of  $q_{max}$  suggesting that PA-AC-HO is a promising adsorbent for removal of MG under the studied conditions. Moreover, the value of  $K_L$  increases with increasing temperature showing endothermic nature of MG adsorption.

The viability of Langmuir isotherm was estimated by an important dimensionless equilibrium parameter which is known as separation factor  $R_L$ , defined by Weber and his coworkers, which can be expressed [44] as:

$$R_L = \frac{1}{1 + K_L C_o} \quad (17)$$

where  $C_o$  (mg L<sup>-1</sup>) is the initial concentration of MG and  $K_L$  is Langmuir constant. The value of  $R_L$  decide whether the Langmuir isotherm is favorable ( $0 < R_L < 1$ ) i.e lies between 0 and 1, unfavorable ( $R_L > 1$ ), linear ( $R_L = 1$ ), or irreversible ( $R_L = 0$ ) [45]. In this study, the values of  $R_L$  for each of the different initial concentrations and temperature lies between 0 and 1, as shown by the plot of  $R_L$  vs.  $C_o$  (Fig. 4(f)), indicating favorable adsorption of MG onto

PA-AC-HO. This confirmed that Langmuir isotherm model fitted well the equilibrium adsorption data. Moreover, at high temperatures,  $R_L$  have much smaller values which showed that MG adsorption is more effective at higher temperatures.

Freundlich isotherm model is an empirical equation, assumes multi-layer adsorption on heterogeneous surfaces with uneven distribution of adsorption heat. The linear form of Freundlich isotherm can be expressed [46] as:

$$\ln q_e = \ln K_F + \frac{1}{n} C_e \quad (18)$$

where  $K_F$  (mg g<sup>-1</sup> (L mg<sup>-1</sup>)<sup>1/n</sup>) and  $1/n$  are Freundlich constants, related to adsorption capacity and adsorption intensity, respectively. The value of  $1/n$  is important as it gives information about the favorability of adsorption reactions. The value of  $1/n$  smaller than 1.0 showed favorable adsorption [47]. The values of isotherm constants  $K_F$  (mg g<sup>-1</sup> (L mg<sup>-1</sup>)<sup>1/n</sup>) and  $1/n$  were determined from the slope and intercept of the liner plots of  $\ln q_e$  vs.  $\ln C_e$  (Fig. 4(c)) and are listed in Table 5. The smaller  $R^2$  value showed that the Freundlich model fit was not as good as Langmuir isotherm for analyzing adsorption data under the given conditions of temperature. The values of  $1/n$  were less than unity, suggesting favorable adsorption of MG onto PA-AC-HO at all studied temperatures.

Temkin isotherm model is based on the assumption that the energy of adsorption linearly decreases with surface coverage due to adsorbate-adsorbent interactions. The linear form of Temkin isotherm model can be expressed as [48]:

$$q_e = \frac{RT}{b_T} \ln K_T + \frac{RT}{b_T} \ln C_e \quad (19)$$

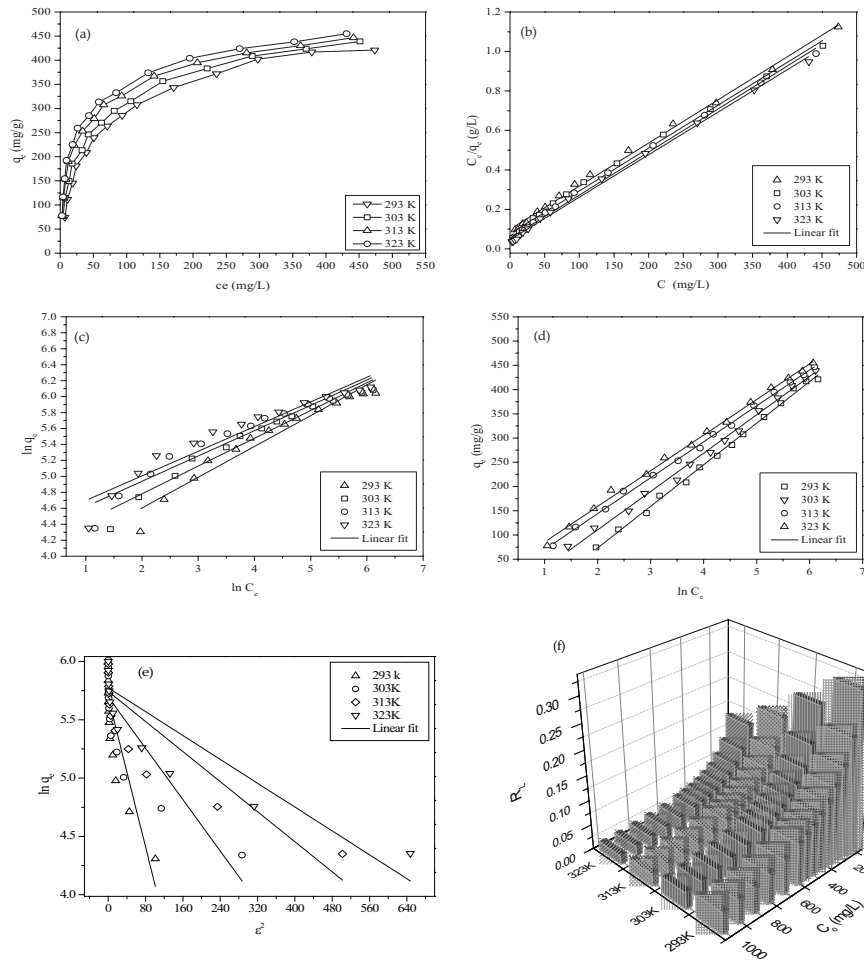


Fig. 4. (a) Adsorption equilibrium, (b) Langmuir, (c) Freundlich, (d) Temkin, (e) D-R isotherms models plots for MG adsorption at different temperature and (f) Variation of  $R_L$  as a function of dye initial concentrations by adsorption onto PA-AC-HO.; PA-AC-HO dosage = 1.25 g L<sup>-1</sup>, pH = 7.0, and speed = 120 rpm.

Table 5  
Isotherms parameters for the adsorption of MG onto PA-AC-HO at different temperatures

Isotherm	Parameters	Temperature (K)			
		293	303	313	323
–	$q_{max,exp}$ (mg g <sup>-1</sup> )	421.10	438.92	446.66	454.94
Langmuir	$q_{max}$ (mg g <sup>-1</sup> )	454.55	454.55	454.55	454.55
	$K_L$ (L mg <sup>-1</sup> )	0.02	0.03	0.04	0.05
	$R^2$	0.99	0.99	0.99	0.99
	$R_L$	0.31	0.26	0.20	0.15
Freundlich	$K_F$ (mg g <sup>-1</sup> (L mg <sup>-1</sup> ) <sup>1/n</sup> )	46.21	59.47	74.04	80.69
	1/n	0.39	0.35	0.32	0.31
	$R^2$	0.95	0.96	0.94	0.93
Temkin	$K_T$ (L mg <sup>-1</sup> )	0.32	0.94	0.94	1.17
	$b_T$ (J mol <sup>-1</sup> )	28.38	31.84	35.11	36.49
	$R^2$	0.99	0.99	0.99	0.99
D-R	$q_{D-R}$ (mg g <sup>-1</sup> )	296.90	297.76	312.22	322.02
	$\beta$ (10 <sup>-6</sup> ) (mol <sup>2</sup> J <sup>-2</sup> )	0.20	6.00	3.00	3.00
	$E$ (kJ mol <sup>-1</sup> )	0.16	0.29	0.41	0.41
	$R^2$	0.73	0.68	0.74	0.77

where  $K_T$  is the equilibrium constant related to the maximum binding energy ( $\text{L g}^{-1}$ ), and the constant  $b_T$  correspond to heat of adsorption ( $\text{J mol}^{-1}$ ) while ' $R$ ' is universal gas constant ( $8.314 \text{ J mol}^{-1} \text{ K}^{-1}$ ) and  $T$  is absolute temperature (K) [9]. The values of Temkin isotherm constants,  $K_T$  and  $b_T$  for the adsorption of MG were determined from the slopes and intercepts of the linear plots of  $q_e$  vs.  $\ln C_e$ , respectively (Fig. 4(d)) and the results are summarized in Table 5. The high  $R^2$  values showed that the Temkin isotherm model also fitted the experimental data very well. The value of  $b_T$  and  $K_T$  was found to increase from 28.33 to 36.49  $\text{J mol}^{-1}$  and 0.32 to 1.17  $\text{L mg}^{-1}$  respectively, with increasing temperature from 298 to 323 K. This effect is because of the increase of surface coverage due to adsorbate-adsorbent interactions and endothermic nature of dye adsorption [49].

The Dubinin-Radushkevich isotherm can be explained by the mathematical expression [50] as:

$$\ln q_e = \ln q_{D-R} - \beta \varepsilon^2 \quad (20)$$

where constant  $q_{D-R}$  is theoretical isotherm adsorption capacity ( $\text{mg g}^{-1}$ ),  $\beta$  is related to the mean free energy of adsorption ( $\text{mol}^2 \text{ J}^{-2}$ ) and  $\varepsilon$  is the Polanyi potential given with  $\varepsilon = RT \ln(1 + 1/C_e)$ . The mean free energy  $E$  ( $\text{kJ mol}^{-1}$ ) can be obtained from the equations as bellow:

$$E = \frac{1}{\sqrt{2\beta}} \quad (21)$$

D-R isotherm constants  $q_{D-R}$  and  $\beta$  were obtained from the slope and intercept of  $\ln q_e$  vs.  $\varepsilon^2$  plots (Fig. 4(e)) and the values obtained are listed in Table 5. The low correlation coefficient ( $\geq 0.68$ ) suggests that D-R model did not fit well the data but the adsorption energy ( $E$ ) value is helpful in predicting adsorption mechanism. The values of  $E$  for the adsorption of MG onto PA-AC-HO were found to be 0.16, 0.29 and 0.41  $\text{kJ mol}^{-1}$  at temperature of 293, 303 and 313 K respectively, are less than 8  $\text{kJ mol}^{-1}$  shows that adsorption of MG onto PA-AC-HO was observed as physisorption due to electrostatic or Van Der Waals interactions [50].

### 3.2.8. Thermodynamic study of adsorption

To determine the feasibility and nature of MG adsorption onto PA-AC-HO at different temperatures, thermodynamic parameters such as  $\Delta G^\circ$ ,  $\Delta H^\circ$  and  $\Delta S^\circ$  have been evaluated by using the following equations [51].

$$\ln K_L = \frac{\Delta H^\circ}{RT} + \frac{\Delta S^\circ}{R} \quad (22)$$

$$\Delta G^\circ = \Delta H^\circ - T\Delta S^\circ \quad (23)$$

where  $R$  ( $8.314 \text{ J mol}^{-1} \text{ K}^{-1}$ ) is the gas constant,  $T$  (K), absolute temperature and  $K_L$  ( $\text{L mg}^{-1}$ ), equilibrium Langmuir constant. The  $\Delta H^\circ$  and  $\Delta S^\circ$  values were calculated respectively, from the slopes and intercepts of the liner plots

Table 6

Thermodynamic parameters for adsorption of MG onto PA-AC-HO at different temperatures

$T$ (K)	$\Delta G^\circ$ ( $\text{kJ mol}^{-1}$ )	$\Delta H^\circ$ ( $\text{J mol}^{-1}$ )	$\Delta S^\circ$ ( $\text{J mol}^{-1} \text{ K}^{-1}$ )
293	-14.75	24.13	50.44
303	-15.26		
313	-15.76		
323	-16.27		

of  $\ln K_L$  vs.  $1/T$  and are summarized in Table 6. It can be seen that  $\Delta H^\circ$  have positive values, showing endothermic nature of adsorption which represents that adsorption capacities of MG increased with rising temperature from 293 to 323 K. The positive  $\Delta S^\circ$  values indicate an increase in the randomness at the solid-solution interface during the uptake process which shows good affinity of MG toward PA-AC-HO surface [52]. At all the studied temperatures, the negative values of  $\Delta G^\circ$  show that the adsorption of MG by PA-AC-HO is feasible and spontaneous in nature. A more negative value of  $\Delta G^\circ$  showed an adsorption process which was favorable energetically. The values of  $\Delta G^\circ$  decreases with rise in temperature from 293 to 323 K, indicates that the affinity of PA-AC-HO was much higher at elevated temperature. Similar findings have been reported by Salima et al [53] for cationic dyes adsorption using activated carbon as adsorbent.

### 3.2.9. Probable adsorption mechanism

The mechanism of dyes uptakes depends on their properties and on the texture and chemistry of adsorbent. The results shows that the possible mechanisms involve in the uptake of MG by PA-AC-HO are electrostatic interaction, H-bonding, pore filling and  $\pi$ - $\pi$  interactions as can be seen in Fig. 5. At pH greater than  $\text{pH}_{\text{PZC}}$  the electrostatic interaction can be the dominant process as evident from Eqs. (6) and (7). However, Weber and Morris intra-particle diffusion model showed that film diffusion and intra-particle also plays dominant role in the adsorption process. H-bonding between the N-atoms of dye cations and the hydrogen atom of carboxylic or phenolic groups of PA-AC-HO and the  $\pi$ - $\pi$  interactions between the  $\pi$  electrons of PA-AC-HO and that of the aromatic rings of dye may also play a role in MG uptakes. The FTIR spectra of dye loaded PA-AC-HO (Fig. 1(d)) shows that the peak of -OH group at  $3732 \text{ cm}^{-1}$  shifted and a low intensity peak at  $3712 \text{ cm}^{-1}$  show the formation of hydrogen bonding between MG and the phenolic groups present on PA-AC-HO surface [2]. After MG uptake the band for C=C absorption shifted from  $1540$  to  $1553 \text{ cm}^{-1}$ . This shifting to upper wavenumber region indicates the presence of  $\pi$ - $\pi$  interactions between dye aromatic rings and the graphitic layer of the adsorbent [54]. These investigation shows that the adsorption of MG by PA-AC-HO involve different pathways such as, electrostatic interactions, pore filling, H-bonding and  $\pi$ - $\pi$  interactions. But the results from pH dependent adsorption (Fig. 2(a)) and Weber-Morris intra-particle diffusion model showed that electrostatic interactions, film diffusion and pore filling plays dominant role.

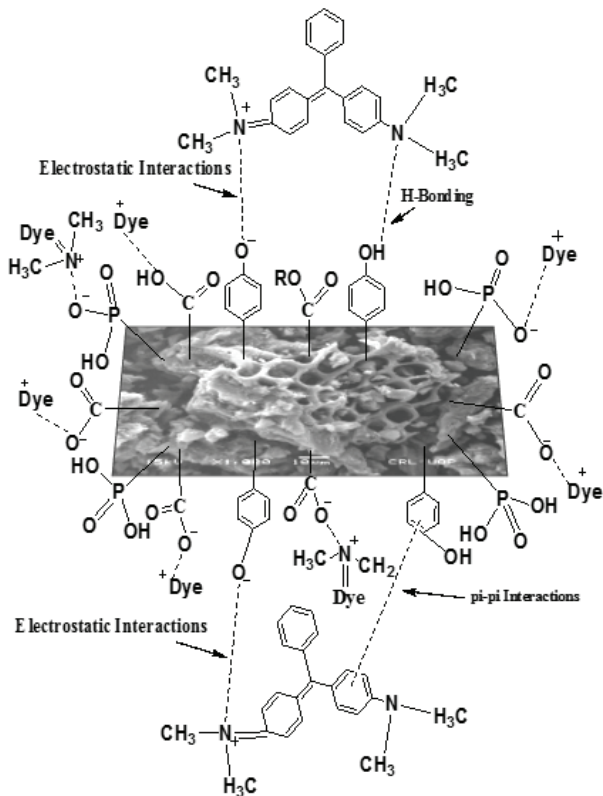


Fig. 5. Probable Mechanism of MG adsorption by PA-AC-HO at optimum pH.

### 3.2.10. Desorption and regeneration of adsorbent

Regeneration of adsorbent is an essential step in wastewater treatment process as it helps in investigating the possible reuse of adsorbent and also provides information about mechanism of adsorption process. Desorption of MG from the surface of PA-AC-HO was studied by batch method by considering the effect of medium pH (2–12), HCl concentrations (0.01–1.0 mol L<sup>-1</sup>) and eluents type (HCl, H<sub>2</sub>SO<sub>4</sub>, HNO<sub>3</sub>, EtOH, NaCl, NaOH and 5% (v/v) EtOH- HCl solution). Results showed that medium pH, eluent type and HCl concentration has considerable effect on MG desorption. Maximum percent desorption was achieved in acidic medium while in basic medium a significant drop in percent desorption was observed (Fig. 6(a)). The highest desorption efficiency in acidic conditions shows that adsorption of MG may involve various types of electrostatic interactions with the functional groups present on the surface of PA-AC-HO [55]. Percent desorption was found to be increased from 0.11% to 46.46% with decreasing desorption medium pH from 12 to 2.0. Similarly, eluents type has also considerable effect on MG desorption and maximum elution was achieved when a 5% (v/v) EtOH- HCl solution was used as eluent, this is then followed by HCl (0.1M), H<sub>2</sub>SO<sub>4</sub> (0.1M), HNO<sub>3</sub> (0.1M), EtOH (10% (v/v)), NaCl (0.1M), and NaOH (0.1M) (Fig. 6(b)). Desorption efficiency was further explored at various concentrations of HCl (Fig. 6(c)). Optimum elution (53.43%) was attained with 0.1 M HCl solution and no significant changes in elution was observed beyond 0.1 M.

Regeneration of PA-AC-HO after saturation with MG was carried out by batch method for five successive cycles

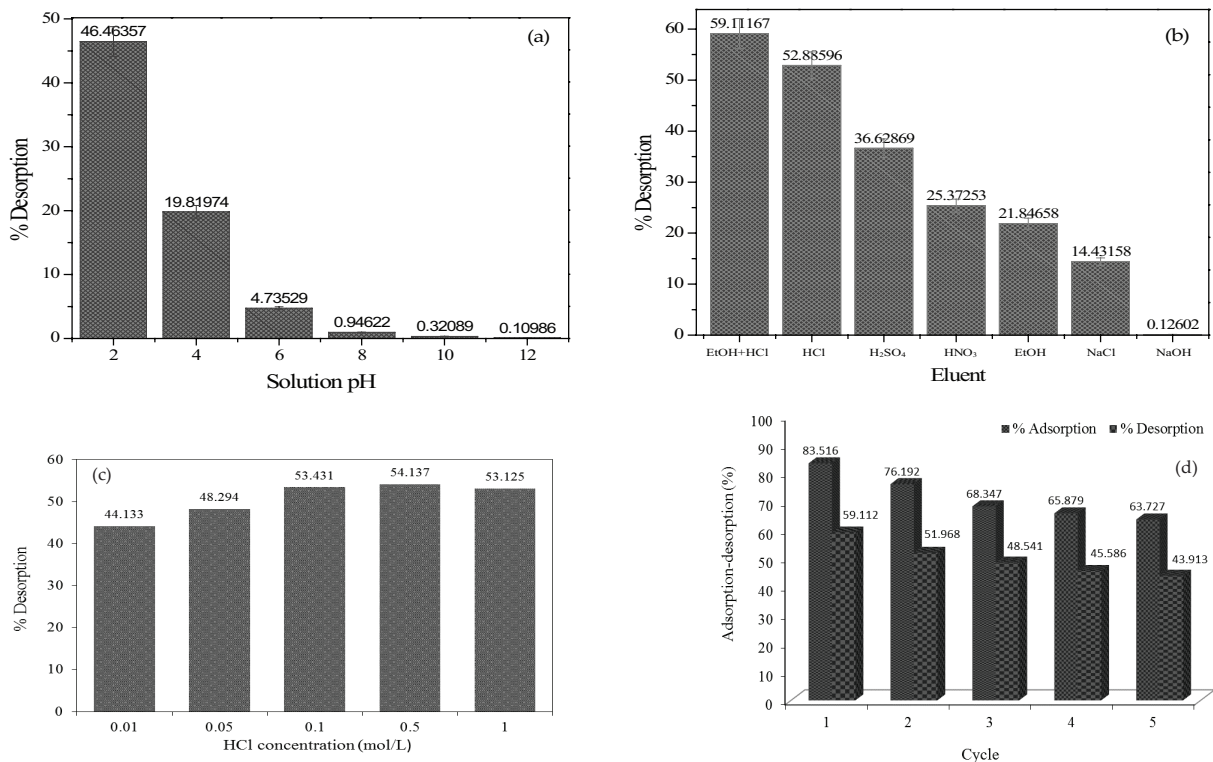


Fig. 6. (a) Effect of medium pH (b) eluents type (c) HCl concentration on desorption of MG and (d) Regeneration and reusability of PA-AC-HO using 5% (V/V) EtOH in 0.1 mol L<sup>-1</sup> HCl solution by five adsorption-desorption cycles.

Table 7

Comparison of maximum adsorption capacity ( $q_{\max}$ ) of MG uptake by PA-AC-HO with other adsorbents

Adsorbent	$q_{\max}$ (mg g <sup>-1</sup> )	References
Almond gum	172.41	[57]
AC loaded with copeer nanoparticle (Cu-NWs-AC)	434.80	[58]
Acid treated sintering red mud (ASRM)	336.40	[2]
Carrot stem powder (CSP)	43.40	[59]
Spent tea AC (STAC)	256.40	[60]
Rambutan peel AC	329.49	[61]
Modified Glossogyne tenuifolia leaves	370.40	[62]
Forestry waste mixture	55.69	[63]
CO <sub>2</sub> -activated porous carbon	276.24	[64]
Tetraethylenepentamine-functionalized activated carbon	333.33	[45]
Nano zero valent iron	187.30	[65]
Stacked activated carbon (NZVI-AC)		
PA-AC-HO	454.55	This study

using a 5% (v/v) EtOH- HCl solution as shown in Fig. 6(d). Results show that sorption efficiency of PA-AC-HO was decreased from 83.52% to 68.35% in the third cycle. In fourth and fifth cycles only a small decrease was observed in percent adsorption which shows that PA-AC-HO could be efficiently reused for dyes adsorption. The significant decrease in adsorption capacity in second and third cycles may be due to loss of some functional groups or active sites on PA-AC-HO surface caused by acidic medium [56].

### 3.2.11. Comparison with other adsorbents

The maximum uptake capacities ( $q_{\max}$ ) of PA-AC-OH utilized in this study for adsorption of MG were compared with many other adsorbents reported in literature, as given in Table 7. It can be observed that PA-AC-OH has sufficiently high adsorption capacity for MG than those reported in the already available literature. This revealed that activated carbon surface modification with H<sub>2</sub>O<sub>2</sub> can provide adsorbent material with high efficiency for the removal of cationic dye (MG) from aqueous systems in the pH range of 4–10.

## 4. Conclusion

PA-AC-HO was efficiently used as a novel adsorbent for the removal of cationic dye, MG from wastewater. SEM micrographs indicated that PA-AC-HO has well developed porous structure with good BET surface area (1,097.68 m<sup>2</sup> g<sup>-1</sup>) and pore volume (0.83 cm<sup>3</sup> g<sup>-1</sup>). The adsorbent surface has high concentration of carboxylic and phenolic groups with the p*H*<sub>PZC</sub> value (3.40) lies in the acidic region. The XRD results showed amorphous nature of PA-AC-HO with high carbon and low ash and volatile matter content which make it high-quality adsorbent for removal of cationic dyes from aqueous systems. The MG adsorption capacity and rate was observed to increase with increasing contact time, dye initial concentrations and solution pH, but showed a declined trend with increasing salt ionic strength. Kinetic results showed that adsorption process follows pseudo-second-order kinetic. The equilibrium data

were well described by Langmuir and Temkin isotherms and the maximum monolayer adsorption capacity was found to be 454.55 mg g<sup>-1</sup>. Adsorption energy (E) values determined from D-R model at different temperatures were less than 8 kJ mol<sup>-1</sup> indicates that MG uptake by PA-AC-HO is physical process involving electrostatic or van der Waals interactions. The values of separation factor ( $R_L$ ) lies between 0 and 1, confirming that PA-AC-HO can be used for effective adsorption of MG from aqueous solutions. Thermodynamic studies depict endothermic, spontaneous and feasible adsorption of dye at all the studied temperatures. In brief, PA-AC-HO can be used as a cleaner and effective adsorbent for detoxification of dyes bearing wastewater, as it has higher adsorption capacity than many other activated carbons and agricultural waste base adsorbents reported in the literature.

## Acknowledgment

Authors are gratified to acknowledge the help and support provided by the National Center of Excellence in Physical Chemistry, University of Peshawar, Pakistan for completing the research project.

## References

- [1] G. Sharma, M. Naushad, A. Kumar, S. Rana, S. Sharma, A. Bhatnagar, F.J. Stadler, A.A. Ghfar, M.R. Khan, Efficient removal of coomassie brilliant blue R-250 dye using starch/poly (alginate acid-cl-acrylamide) nanohydrogel, *Process. Saf. Environ. Protect.*, 109 (2017) 301–310.
- [2] L. Zhang, H. Zhang, W. Guo, Y. Tian, Removal of malachite green and crystal violet cationic dyes from aqueous solution using activated sintering process red mud, *Appl. Clay Sci.*, 93 (2014) 85–93.
- [3] T. Santhi, S. Manonmani, T. Smitha, Removal of malachite green from aqueous solution by activated carbon prepared from the epicarp of *Ricinus communis* by adsorption, *J. Hazard. Mater.*, 179 (2010) 178–186.
- [4] A.B. Albadarin, M. Charara, B.J.A. Tarboush, M. Ahmad, T.A. Kurniawan, M. Naushad, G.M. Walker, C. Mangwandi, Mechanism analysis of tartrazine biosorption onto masau stones; a low cost by-product from semi-arid regions, *J. Mole. Liq.*, 242 (2017) 478–483.

- [5] G. Sharma, A. Kumar, M. Naushad, A. García-Peñas, H. Ala'a, A.A. Ghfar, V. Sharma, T. Ahamad, F.J. Stadler, Fabrication and characterization of Gum arabic-*cl*-poly (acrylamide) nanohydrogel for effective adsorption of crystal violet dye, *Carbohydr. polym.*, 202 (2018) 444–453.
- [6] K.-W. Jung, B.H. Choi, M.-J. Hwang, T.-U. Jeong, K.-H. Ahn, Fabrication of granular activated carbons derived from spent coffee grounds by entrapment in calcium alginate beads for adsorption of acid orange 7 and methylene blue, *Bioresour. Technol.*, 219 (2016) 185–195.
- [7] V. Gupta, A. Mittal, L. Krishnan, V. Gajbe, Adsorption kinetics and column operations for the removal and recovery of malachite green from wastewater using bottom ash, *Sep. Purif. Technol.*, 40 (2004) 87–96.
- [8] Y. Kan, Q. Yue, J. Kong, B. Gao, Q. Li, The application of activated carbon produced from waste printed circuit boards (PCBs) by  $H_3PO_4$  and steam activation for the removal of malachite green, *Chem. Eng. J.*, 260 (2015) 541–549.
- [9] C. Pearce, J. Lloyd, J. Guthrie, The removal of colour from textile wastewater using whole bacterial cells: a review, *Dyes. Pigm.*, 58 (2003) 179–196.
- [10] J.S. da Silva, M.P. da Rosa, P.H. Beck, E.C. Peres, G.L. Dotto, F. Kessler, F.S. Grasel, Preparation of an alternative adsorbent from *Acacia Mearnsii* wastes through acetosolv method and its application for dye removal, *J. Cleaner. Prod.*, 180 (2018) 386–394.
- [11] M. Naushad, Z. Al-Othman, M. Islam, Adsorption of cadmium ion using a new composite cation-exchanger polyaniline Sn (IV) silicate: kinetics, thermodynamic and isotherm studies, *Int. J. Environ. Sci. Technol.*, 10 (2013) 567–578.
- [12] J. Georjgin, G.L. Dotto, M.A. Mazutti, E.L. Foletto, Preparation of activated carbon from peanut shell by conventional pyrolysis and microwave irradiation-pyrolysis to remove organic dyes from aqueous solutions, *J. Environ. Chem. Eng.*, 4 (2016) 266–275.
- [13] A.A. Alqadami, M. Naushad, M.A. Abdalla, T. Ahamad, Z.A. AlOthman, S.M. Alshehri, A.A. Ghfar, Efficient removal of toxic metal ions from wastewater using a recyclable nanocomposite: a study of adsorption parameters and interaction mechanism, *J. Cleaner. Prod.*, 156 (2017) 426–436.
- [14] Z.A. Al-Othman, R. Ali, M. Naushad, Hexavalent chromium removal from aqueous medium by activated carbon prepared from peanut shell: adsorption kinetics, equilibrium and thermodynamic studies, *Chem. Eng. J.*, 184 (2012) 238–247.
- [15] S. Wang, Z. Zhu, A. Coomes, F. Haghseresht, G. Lu, The physical and surface chemical characteristics of activated carbons and the adsorption of methylene blue from wastewater, *J. Colloid. Interface. Sci.*, 284 (2005) 440–446.
- [16] Y. Gokce, Z. Aktas, Nitric acid modification of activated carbon produced from waste tea and adsorption of methylene blue and phenol, *App. Surf. Sci.*, 313 (2014) 352–359.
- [17] E. El-Shafey, S.N. Ali, S. Al-Busafi, H.A. Al-Lawati, Preparation and characterization of surface functionalized activated carbons from date palm leaflets and application for methylene blue removal, *J. Environ. Chem. Eng.*, 4 (2016) 2713–2724.
- [18] X. Zuo, Z. Liu, M. Chen, Effect of  $H_2O_2$  concentrations on copper removal using the modified hydrothermal biochar, *Bioresour. Technol.*, 207 (2016) 262–267.
- [19] M.F.R. Pereira, S.F. Soares, J.J. Órfão, J.L. Figueiredo, Adsorption of dyes on activated carbons: influence of surface chemical groups, *Carbon*, 41 (2003) 811–821.
- [20] T. Mahmood, R. Ali, A. Naeem, M. Hamayun, M. Aslam, Potential of used *Camellia sinensis* leaves as precursor for activated carbon preparation by chemical activation with  $H_3PO_4$ ; optimization using response surface methodology, *Process Saf. Environ. Prot.*, 109 (2017) 548–563.
- [21] E.P. Barrett, L.G. Joyner, P.P. Halenda, The determination of pore volume and area distributions in porous substances. I. Computations from nitrogen isotherms, *J. Am. Chem. Soc.*, 73 (1951) 373–380.
- [22] M. Dubinin, *Progress in Surface and Membrane*, vol. 9, Academic, New York. (1975).
- [23] F. Rodriguez-Reinoso, M. Molina-Sabio, M. Gonzalez, The use of steam and  $CO_2$  as activating agents in the preparation of activated carbons, *Carbon*, 33 (1995) 15–23.
- [24] H. Boehm, Surface oxides on carbon and their analysis: a critical assessment, *Carbon*, 40 (2002) 145–149.
- [25] M. Benadjemia, L. Millière, L. Reinert, N. Benderdouche, L. Duclaux, Preparation, characterization and Methylene Blue adsorption of phosphoric acid activated carbons from globe artichoke leaves, *Fuel. Process. Technol.*, 92 (2011) 1203–1212.
- [26] X. Song, H. Liu, L. Cheng, Y. Qu, Surface modification of coconut-based activated carbon by liquid-phase oxidation and its effects on lead ion adsorption, *Desalination*, 255 (2010) 78–83.
- [27] J. Jaramillo, P.M. Álvarez, V. Gómez-Serrano, Oxidation of activated carbon by dry and wet methods: surface chemistry and textural modifications, *Fuel. Process. Technol.*, 91 (2010) 1768–1775.
- [28] E.G. Lemraski, S. Sharafinia, Kinetics, equilibrium and thermodynamics studies of  $Pb^{2+}$  adsorption onto new activated carbon prepared from Persian mesquite grain, *J. Mol. Liq.*, 219 (2016) 482–492.
- [29] A. Shahat, M.R. Awual, M.A. Khaleque, M.Z. Alam, M. Naushad, A.S. Chowdhury, Large-pore diameter nano-adsorbent and its application for rapid lead (II) detection and removal from aqueous media, *Chem. Eng. J.*, 273 (2015) 286–295.
- [30] C. Chen, X. Li, Z. Tong, Y. Li, M. Li, Modification process optimization, characterization and adsorption property of granular fir-based activated carbon, *Appl. Surf. Sci.*, 315 (2014) 203–211.
- [31] R.M. Silverstein, F.X. Webster, D.J. Kiemle, D.L. Bryce, *Spectrometric identification of organic compounds*, John Wiley & Sons, 2014.
- [32] H. Guedidi, L. Reinert, J.-M. Lévêque, Y. Soneda, N. Bellakhal, L. Duclaux, The effects of the surface oxidation of activated carbon, the solution pH and the temperature on adsorption of ibuprofen, *Carbon*, 54 (2013) 432–443.
- [33] M.O. Guerrero-Pérez, J.M. Rosas, R. López-Medina, M.A. Bañares, J. Rodríguez-Mirasol, T. Cordero, Lignocellulosic-derived catalysts for the selective oxidation of propane, *Catal. Commun.*, 12 (2011) 989–992.
- [34] A. Saeed, M. Sharif, M. Iqbal, Application potential of grapefruit peel as dye sorbent: kinetics, equilibrium and mechanism of crystal violet adsorption, *J. Hazard. Mater.*, 179 (2010) 564–572.
- [35] L. Ding, B. Zou, W. Gao, Q. Liu, Z. Wang, Y. Guo, X. Wang, Y. Liu, Adsorption of Rhodamine-B from aqueous solution using treated rice husk-based activated carbon, *Colloid. Surf., A.*, 446 (2014) 1–7.
- [36] M. Goswami, P. Phukan, Enhanced adsorption of cationic dyes using sulfonic acid modified activated carbon, *J. Environ. Chem. Eng.*, 5 (2017) 3508–3517.
- [37] K. Vermöhlen, H. Lewandowski, H.-D. Narres, M. Schwuger, Adsorption of polyelectrolytes onto oxides—the influence of ionic strength, molar mass, and  $Ca^{2+}$  ions, *Colloid. Surf., A.*, 163 (2000) 45–53.
- [38] R. Han, W. Zou, W. Yu, S. Cheng, Y. Wang, J. Shi, Biosorption of methylene blue from aqueous solution by fallen phoenix tree's leaves, *J. Hazard. Mater.*, 141 (2007) 156–162.
- [39] G. Manikandan, S. Kumar, A. Saravanan, Modelling and analysis on the removal of methylene blue dye from aqueous solution using physically/chemically modified *Ceiba pentandra* seeds, *J. Ind. Eng. Chem.*, 62 (2018) 446–461.
- [40] E. Daneshvar, A. Vazirzadeh, A. Niazi, M. Sillanpää, A. Bhatnagar, A comparative study of methylene blue biosorption using different modified brown, red and green macroalgae—effect of pretreatment, *Chem. Eng. J.*, 307 (2017) 435–446.
- [41] S. Banerjee, M. Chattopadhyaya, Adsorption characteristics for the removal of a toxic dye, tartrazine from aqueous solutions by a low cost agricultural by-product, *Arab. J. Chem.*, 10 (2017) S1629–S1638.
- [42] S. Kaur, S. Rani, R. Mahajan, M. Asif, V.K. Gupta, Synthesis and adsorption properties of mesoporous material for the removal of dye safranin: kinetics, equilibrium, and thermodynamics, *J. Ind. Eng. Chem.*, 22 (2015) 19–27.

- [43] M. Ghaedi, A. Ansari, M. Habibi, A. Asghari, Removal of malachite green from aqueous solution by zinc oxide nanoparticle loaded on activated carbon: kinetics and isotherm study, *J. Ind. Eng. Chem.*, 20 (2014) 17–28.
- [44] A.B. Albadarin, M.N. Collins, M. Naushad, S. Shirazian, G. Walker, C. Mangwandi, Activated lignin-chitosan extruded blends for efficient adsorption of methylene blue, *Chem. Eng. J.*, 307 (2017) 264–272.
- [45] M. Ghasemi, S. Mashhadi, M. Asif, I. Tyagi, S. Agarwal, V.K. Gupta, Microwave-assisted synthesis of tetraethylenepentamine functionalized activated carbon with high adsorption capacity for Malachite green dye, *J. Mol. Liq.*, 213 (2016) 317–325.
- [46] M. Naushad, Surfactant assisted nano-composite cation exchanger: development, characterization and applications for the removal of toxic  $Pb^{2+}$  from aqueous medium, *Chem. Eng. J.*, 235 (2014) 100–108.
- [47] P.K. Malik, Dye removal from wastewater using activated carbon developed from sawdust: adsorption equilibrium and kinetics, *J. Hazard. Mater.*, 113 (2004) 81–88.
- [48] V.S. Mane, I.D. Mall, V.C. Srivastava, Kinetic and equilibrium isotherm studies for the adsorptive removal of Brilliant Green dye from aqueous solution by rice husk ash, *J. Environ. Manage.*, 84 (2007) 390–400.
- [49] A. Jalil, S. Triwahyono, M. Yaakob, Z. Azmi, N. Sapawe, N. Kamarudin, H. Setiabudi, N. Jaafar, S. Sidik, S. Adam, Utilization of bivalve shell-treated *Zea mays* L. (maize) husk leaf as a low-cost biosorbent for enhanced adsorption of malachite green, *Bioresour. Technol.*, 120 (2012) 218–224.
- [50] C. Muthukumar, V.M. Sivakumar, M. Thirumarimurugan, Adsorption isotherms and kinetic studies of crystal violet dye removal from aqueous solution using surfactant modified magnetic nano-adsorbent, *J. Taiwan. Inst. Chem. Eng.*, 63 (2016) 354–362.
- [51] P. Rai, R.K. Gautam, S. Banerjee, V. Rawat, M. Chattopadhyaya, Synthesis and characterization of a novel  $SnFe_2O_4@$  activated carbon magnetic nanocomposite and its effectiveness in the removal of crystal violet from aqueous solution, *J. Environ. Chem. Eng.*, 3 (2015) 2281–2291.
- [52] N. Tahir, H.N. Bhatti, M. Iqbal, S. Noreen, Biopolymers composites with peanut hull waste biomass and application for Crystal Violet adsorption, *Int. J. Biolo. Macromol.*, 94 (2017) 210–220.
- [53] A. Salima, B. Benaouda, B. Noureddine, L. Duclaux, Application of *Ulva lactuca* and *Systoceira stricta* algae-based activated carbons to hazardous cationic dyes removal from industrial effluents, *Water. Res.*, 47 (2013) 3375–3388.
- [54] H.N. Tran, S.-J. You, H.-P. Chao, Fast and efficient adsorption of methylene green 5 on activated carbon prepared from new chemical activation method, *J. Environ. Manage.*, 188 (2017) 322–336.
- [55] E. Daneshvar, A. Vazirzadeh, A. Niazi, M. Kousha, M. Naushad, A. Bhatnagar, Desorption of Methylene blue dye from brown macroalga: effects of operating parameters, isotherm study and kinetic modeling, *J. Clean. Prod.*, 152 (2017) 443–453.
- [56] M.R. Malekbala, M.A. Khan, S. Hosseini, L.C. Abdullah, T.S. Choong, Adsorption/desorption of cationic dye on surfactant modified mesoporous carbon coated monolith: equilibrium, kinetic and thermodynamic studies, *J. Ind. Eng. Chem.*, 21 (2015) 369–377.
- [57] F. Bouaziz, M. Koubaa, F. Kallel, R.E. Ghorbel, S.E. Chaabouni, Adsorptive removal of malachite green from aqueous solutions by almond gum: kinetic study and equilibrium isotherms, *Int. J. Biol. Macromol.*, 105 (2017) 56–65.
- [58] M. Ghaedi, S. Khodadoust, H. Sadeghi, M.A. Khodadoust, R. Armand, A. Fatehi, Application of ultrasonic radiation for simultaneous removal of auramine O and safranin O by copper sulfide nanoparticles: experimental design, *Spectrochim. Acta. A. Mol. Biomol. Spectrosc.*, 136 (2015) 1069–1075.
- [59] A.K. Kushwaha, N. Gupta, M. Chattopadhyaya, Removal of cationic methylene blue and malachite green dyes from aqueous solution by waste materials of *Daucus carota*, *J. Saudi. Chem. Soc.*, 18 (2014) 200–207.
- [60] E. Akar, A. Altinişik, Y. Seki, Using of activated carbon produced from spent tea leaves for the removal of malachite green from aqueous solution, *Ecol. Eng.*, 52 (2013) 19–27.
- [61] M.A. Ahmad, R. Alrozi, Removal of malachite green dye from aqueous solution using rambutan peel-based activated carbon: equilibrium, kinetic and thermodynamic studies, *Chem. Eng. J.*, 171 (2011) 510–516.
- [62] J.-X. Yang, G.-B. Hong, Adsorption behavior of modified *Glossogyne tenuifolia* leaves as a potential biosorbent for the removal of dyes, *J. Mol. Liq.*, 252 (2018) 289–295.
- [63] F. Deniz, R.A. Kepekci, Bioremoval of Malachite green from water sample by forestry waste mixture as potential biosorbent, *Microchem. J.*, 132 (2017) 172–178.
- [64] M. Yu, Y. Han, J. Li, L. Wang,  $CO_2$ -activated porous carbon derived from cattail biomass for removal of malachite green dye and application as supercapacitors, *Chem. Eng. J.*, 317 (2017) 493–502.
- [65] P.S. Kumar, S.J. Varjani, S. Suganya, Treatment of dye wastewater using an ultrasonic aided nanoparticle stacked activated carbon: kinetic and isotherm modelling, *Bioresour. Technol.*, 250 (2018) 716–722.